Realizing An Acoustic Vector Network Analyser

Marcus MacDonell[1] and Jonathan Scott[1]

[1]*University of Waikato*

Correspondence should be addressed to Marcus MacDonell (`msgm1@students.waikato.ac.nz`)

ABSTRACT

Acoustic absorption, reflection, and transmission is typically measured using an impedance tube. We present the design and initial measurements of a radically different measurement system. The instrument builds on the rich history and deep mathematics developed in pursuit of electromagnetic Vector-corrected Network Analyzers (VNAs). Using acoustic directional couplers and a traditional VNA mainframe we assembled an "Acoustic Vector Network Analyzer" (AVNA). The instrument measures acoustic scattering parameters, the complex reflection and transmission coefficients, of materials, transmission lines, ported structures, ducts, etc. After the fashion of electromagnetic VNAs we have constructed millimeter-wave measurement heads that span the 800 Hz–2200 Hz (420–150 mm) and 10 kHz–22 kHz (35–15 mm) bands, demonstrating scalability. We present initial measurement results.

1 Introduction

Absorbing materials play an important role in architectural acoustics, the design of recording studios, listening rooms, and automobile interiors. The growth and decay of the reverberant sound field in a room depends on the absorbing properties of the materials used [1–3]. The sound transmission properties of components are also of interest to acoustic engineers. For example, attenuation in ducts impacts the delivery of fan noise, and the loss in pipe-shaped components of musical instruments affects their performance. The acoustic attenuation of material samples placed in a waveguide reflects subtle properties of the material. In this manuscript we describe a new instrument that offers the potential to deliver acoustic reflection and transmission measurements with traceable accuracy and unprecedented measurement speed. The design is inspired by an instrument developed and refined over many decades since the second world war and now

ubiquitous in radio and microwave laboratories all over the world: the Vector-corrected Network Analyzer or "VNA".

A Vector Network Analyzer (VNA) is an instrument that measures the parameters of an electrical network. There is a rich history of their design spanning over 50 years [4]. Vector network analyzers are mostly 'two-port' analyzers that measure two port systems like amplifiers and filters, but single-port and higher order systems with an arbitrary number of ports are possible. Key to the operation of VNAs is the ability to separate waves traveling in opposite directions along a transmission line [5]. This allows the instrument to report reflection coefficient, the ratio of incident to reflected signal. It also enables a mathematically-sophisticated calibration procedure that can negate the effects of imperfections in the instrument itself.

VNAs measure so-called "scattering parameters" or S-parameters [5]. S-parameters are the most commonly

measured parameters because the reflection and transmission coefficients of electrical networks are easy to measure at high frequencies compared with ordinary complex impedance [6].

At present, acoustic measurements to characterize materials are typically done with two industry standard techniques [7, 8]. Neither of these methods is traceable to an external standard. Both are performed frequency by frequency in a laborious manner. The multiple-microphone method can be unreliable especially when phase is important [9]. Other methods in the acoustic domain essentially use an impedance divider in a waveguide [10–13]. None of these methods is particularly precise, and none have become common.

In the early years of radio frequency (RF) test and measurement there were a few techniques available to measure magnitude and phase traveling waves. The slotted line was one of the first techniques that was developed by what is now the company Rohde & Schwarz. The "slotted-line" is the radio frequency equivalent of the moving-microphone method for separation of two acoustic traveling waves propagating in opposite directions. Rantec and Wiltron introduced various Phase-/Gain/amplitude meters/receivers in the 1950s that covered the microwave frequency range. In the 1960s simple Network Analyzers were assembled by mating directional couplers with vector meters. At that time, s-parameters were proposed as a design tool for microwave circuit design and engineering, requiring measurement of the parameters. In the late 1960s the Hewlett-Packard company released the HP 8410, a Network Analyzer without inbuilt error calibration, and began work on vector correction. By the middle of the 1980s the so-called SOLT (Short, Open, Load, Thru) and TRL (Thru, Reflect, Line) calibrations had been proven as mathematically-sound ways of achieving precise calibration; the HP 8510 was introduced to the market as the first instrument with in-built error correction. By the 1990s VNA capability had been extended into the world of optics [14, 15] and on wafer measurement [16, 17] with the added development of LR(R)M calibration techniques [18, 19]. The development of the TRL and TR(R)M calibration methods required fewer standards than SOLT, greatly improved calibration accuracy by allowing weaker standards to be discarded, and extended the number of error terms corrected up to the full 16. Machines were now being sold that spanned the frequency range from below 50MHz (wavelength

of 6m) to over 110GHz (wavelength of 3mm). A wavelength of 6m in the case of sound in air represents a frequency of just over 50Hz, while 3mm corresponds to 110kHz, a very wide range indeed.

The VNA was instrumental in the development of every new generation of radar. It enabled most of the high-frequency electronic systems we enjoy today, including cellular phones, global positioning, WiFi, and ethernet. In all of the VNAs sold, directional couplers are the fundamental building block. Directional couplers in their waveguide form are not dissimilar from one another, and this proves to be true even in the acoustic case. As such it may be surprising to note that the development in 1971 of the acoustic directional coupler [21] was never followed by the serious adoption of VNA techniques in acoustics.
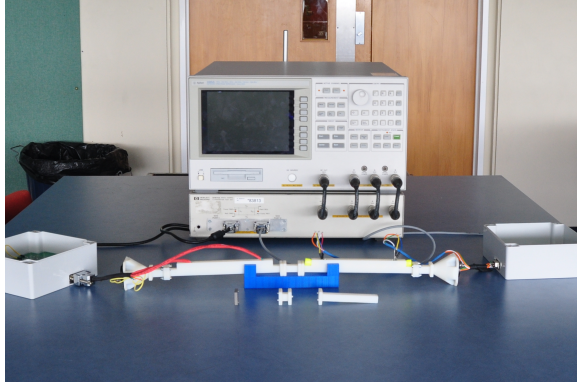
2 Hardware

In an effort to improve on the available acoustic methods, we have constructed a dual-port Acoustic Vector Network Analyser (AVNA) [20]. This is based around Lagasse's coupler design [21]. Figure 1 shows our prototype system consisting of an old HP4395A VNA mainframe fitted with two 3D-printed measurement heads. Figure 2 presents the block diagram of the system; interested readers will find it similar to those of millimetre-wave commercial electro-magnetic VNAs. The physical design also mimics the remote-head, waveguide-based VNA designs offered by companies such as Keysight and Anritsu. Each head incorporates a directional coupler for 10–20 kHz operation [22], within which is a matching pad & sound source [20], and electronics to interface sensing microphones to the VNA receivers. This system will be used here to measure acoustic S-parameters.

Figure 3 depicts an early version of the coupler-pad-source component, conveniently constructed for the 1–2 kHz band, in transparent acrylic to show the internal geometry. In front of that is shown a sliding load and other waveguide components. To the rear of the image a 1-foot (300mm) ruler gives scale.

To further improve this system we report here a system for calibrating our AVNA, and we discuss standards that we anticipate can be made traceable. The reliability and repeatability of the flange system is crucial to the physical performance of the acoustic VNA as well as the performance of any potential calibration

technique, and we have explored this design in some detail elsewhere [23], and incorporated it into all of our hardware.


Fig. 1: The physical hardware for the acoustic vector network analyser. The commercial VNA (rear top) sits atop of a retrofitted 'test-set' which connects the waveguide (front center) via external amplifiers (white boxes on the far left and right).
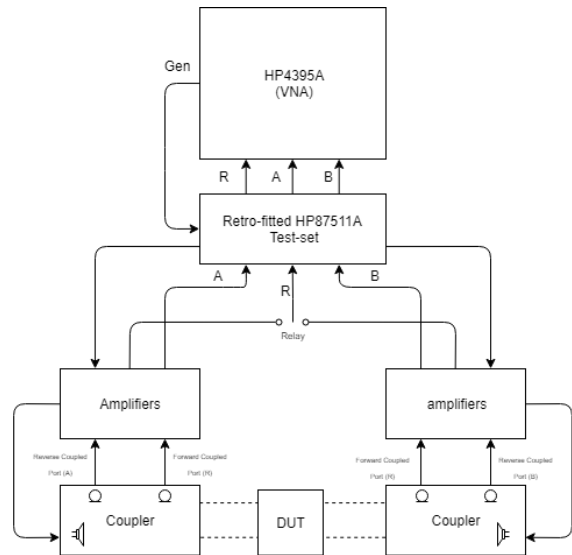
Fig. 2: A block diagram of the hardware presented in Figure 1. The presented configuration is using two ports to measure a "Device Under Test" (DUT).
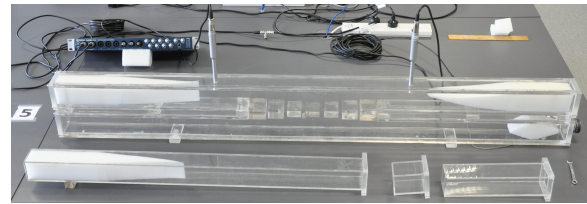
Fig. 3: An example of an acoustic directional coupler for 1–2 kHz, the branch waveguide structure responsible for it's directional behavior is clearly visible thanks to being constructed of colourless polycarbonate. Microphones left and right are the forward and reverse coupled "ports" respectively.
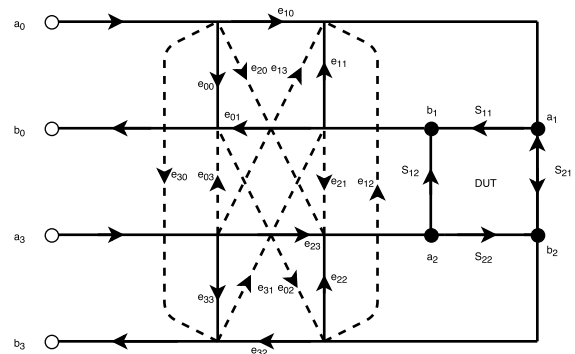
Fig. 4: A flow-graph of the 16 term error model. This flow-graph represents the physical paths for systematic error in the system, these are numerically represented in the error matrix 'E'

3 Calibration Methods

Owing to the imperfections of acoustic directional couplers, the advance of the AVNA depends upon the development of a calibration method. The calibration method is a process for determining the systematic error of the measurement device. A correction algorithm is then applied to convert raw measurements into corrected ones.

The analysis of a VNA is traditionally carried out using traveling-wave flow graphs [24, 25]. The complete 16-term error model represented in flow-graph form is shown in figure 4. Based on the model, a system of equations relating raw to corrected measurements is found. This system of linear equations that relate the measured acoustic properties of a device under test

(DUT) to the actual acoustic properties of the DUT, present a considerable algebraic problem. The act of calibration takes measurements made on known devices, and solves for the 16 error terms. The 16 term error model was chosen because of the inclusion of leakage paths that are expected to be an issue in the acoustic VNA, but that may often be ignored in the electromagnetic case by virtue of Faraday shielding.

We face finding 16 complex error terms. Unfortunately, very few known acoustic standards exist. The most obvious standard is a perfect reflection, consisting of a guide closed with a solid panel. In previous work, it was shown that the so-called "sliding load" method, adapted from a scheme popular in the electromagnetic domain in the 1980s, could provide the equivalent of a perfect absorber [26, 29]. The sliding load works by utilizing the phase change of the reflected signal from an imperfect absorber whose reflection magnitude is invariant at different positions in a guide. The result that would have been obtained from a perfect absorber can be calculated from the value of a imperfect absorber. This is normally done with a numerical circle fit, or possibly a spiral fit. These two standards (Reflect, [sliding] Load) are insufficient by themselves, even for a single port VNA [9].

As we have two ports, it is possible to connect them directly, measuring a so-called "zero-length Thru". With the available 'Thru', 'Match', and 'Reflect' standards we can adapt the LRM or TRRM electromagnetic calibration methods proposed by Silvonen [27] to solve the system. This method utilizes five measurements of combinations of the standards to produce a set of twenty equations. This overdetermined system can be solved with a numerical method like Single Value Decomposition (SVD), or with the analytical results from [27].

3.1 Calibration

The five required measurements have the ideal matrices:

$$\text{Thru:} \quad A = \begin{bmatrix} 0 & T \\ T & 0 \end{bmatrix} \tag{1}$$

$$\text{Match-Match:} \quad B = \begin{bmatrix} 0 & 0 \\ 0 & 0 \end{bmatrix} \tag{2}$$

$$\text{Reflect-Reflect:} \quad C = \begin{bmatrix} \Gamma & 0 \\ 0 & \Gamma \end{bmatrix} \tag{3}$$

$$\text{Reflect-Match:} \quad D = \begin{bmatrix} \Gamma & 0 \\ 0 & 0 \end{bmatrix} \tag{4}$$

$$\text{Match-Reflect:} \quad E = \begin{bmatrix} 0 & 0 \\ 0 & \Gamma \end{bmatrix} \tag{5}$$

For a zero-length Thru $T = 1$, and our method uses a zero-length Thru since it is the simplest option. T is otherwise calculated from its length l and propagation constant γ, where $T = e^{-\gamma l}$, but the (time) length of a thru in the acoustic domain is subject to many uncertainties, not least concerning the variable properties of air. The 16-term error model shown in figure 4 yields the matrix representation in equation (6), expanded in 7. E represents the 16-term error matrix while e represents and individual error term. e_{00} for example represents the error as a result of signal following the path shown in Figure 4 from port a_0 to b_0.

$$\begin{bmatrix} b_0 \\ b_3 \\ b_1 \\ b_2 \end{bmatrix} = E \begin{bmatrix} a_0 \\ a_3 \\ a_1 \\ a_2 \end{bmatrix} \tag{6}$$

$$E \equiv \begin{bmatrix} E_1 & E_2 \\ E_3 & E_4 \end{bmatrix} = \left[\begin{array}{cc:cc} e_{00} & e_{03} & e_{01} & e_{02} \\ e_{30} & e_{33} & e_{31} & e_{32} \\ \hdashline e_{10} & e_{13} & e_{11} & e_{12} \\ e_{20} & e_{23} & e_{21} & e_{22} \end{array} \right] \tag{7}$$

S_m, the "measured" S-parameters and S_a, the "actual" S-parameters are defined as

$$\begin{bmatrix} b_0 \\ b_3 \end{bmatrix} = S_m \begin{bmatrix} a_0 \\ a_3 \end{bmatrix}, \; S_m = \begin{bmatrix} S_{11m} & S_{12m} \\ S_{21m} & S_{22m} \end{bmatrix} \tag{8}$$

$$\begin{bmatrix} a_1 \\ a_2 \end{bmatrix} = S_a \begin{bmatrix} b_1 \\ b_2 \end{bmatrix}, \; S_a = \begin{bmatrix} S_{11a} & S_{12a} \\ S_{21a} & S_{22a} \end{bmatrix} \tag{9}$$

$$S_m = E_1 + E_2 S_a (I - E_4 S_a)^{-1} E_3 \tag{10}$$

Where I is the unit matrix. Solving for S_a yields

$$S_a = [E_3(S_m - E_1)^{-1}E_2 + E_4]^{-1} \qquad (11)$$

This equation is very non-linear and difficult to solve directly. Cascading T-parameters are used to linearize the problem. Solving for the T-parameters can be done in a variety of ways. Two common methods are normalizing by one of the unknown coefficients and solving directly or using a least squares method, single value decomposition (SVD) is used often because of its ability to handle singularities [28].

The E and T matrices are related by the following:

$$E = \begin{bmatrix} T_2 T_4^{-1} & T_1 - T_2 T_4^{-1} T_3 \\ T_4^{-1} & -T_4^{-1} T_3 \end{bmatrix} \qquad (12)$$

$$T = \begin{bmatrix} E_2 E_1 E_3^{-1} E_4 & E_1 T_3^{-1} \\ E_3^{-1} E_4 & E_3^{-1} \end{bmatrix} \qquad (13)$$

Substituting the T matrix into the system yields:

$$\begin{bmatrix} b_0 \\ b_3 \\ a_0 \\ a_3 \end{bmatrix} = T \begin{bmatrix} a_1 \\ a_2 \\ b_1 \\ b_2 \end{bmatrix} \qquad (14)$$

$$T \equiv \begin{bmatrix} T_1 & T_2 \\ T_3 & T_4 \end{bmatrix} = \begin{bmatrix} t_0 & t_1 & t_2 & t_3 \\ t_4 & t_5 & t_6 & t_7 \\ t_8 & t_9 & t_{10} & t_{11} \\ t_{12} & t_{13} & t_{14} & t_{15} \end{bmatrix} \qquad (15)$$

Using the T-parameters and the definitions of S_m and S_a the following can be derived

$$S_m = (T_1 S_a + T_2)(T_3 S_a + T_4)^{-1} \qquad (16)$$

$$T_1 S_a + T_2 - S_m T_3 S_a - S_m T_4 = 0 \qquad (17)$$

$$S_a = (T_1 - S_m T_3)^{-1}(S_m T_4 - T_2) \qquad (18)$$

Equation 17 forms the basis of calibration and can be arranged into the form of $\mathbf{A} \cdot T = 0$ and produces a set of twenty linear equations in terms of the 16 T-parameters t_n. Equation 18 allows for de-embedding of the DUT.

The full system of equations generated by the five measurements is presented for the interested reader in Figure 9 towards the end of this manuscript.

4 Results

Figure 5 shows the corrected data of the 'Thru' (zero-length) standard when using the error matrix produced by the numerical method. This shows that the transmission terms (S_{12} & S_{21}) very well calibrated to 0 dB (100% transmission) with reflections (S_{11} & S_{22}) sitting at least -40 dB down.

Figure 6 shows the the corrected data of the 'reflect' standard when using the error matrix produced by the analytical method. This shows that the reflection terms (S_{11} & S_{22}) very well calibrated to 0 dB (100% reflection) with transmission (S_{12} & S_{21}) down around -350 dB. This is the numerical computation noise, as expected because the calibration is algebraic, rather than numerical.

The performance of the 'Match' standard which is implemented as a sliding load is limited by the performance of the circle fit used. The circle fit used is the Taubin method [30]. In order for this method to work effectively there needs to be sufficient points for the method to fit a least squares solution for all frequencies. Three points are theoretically sufficient, however when implementing the sliding load practically there are frequencies where more points may be required for an accurate fit. Imperfections in the circle fit manifest themselves as an increase in the noise floor, especially where the result is small.

5 Discussion

Once the error matrix has been generated using the analytical and numerical methods, the error matrix can be checked. To check the error matrix is valid mathematically it is multiplied by any set of measured S-parameters for a standard. If the result of this multiplication is the same as the ideal matrix for that standard then the calibration has been successful.

When the SVD and analytic solutions proved results that are in agreement, we may be reasonably sure that there are no errors or bugs in the calibration algorithms.
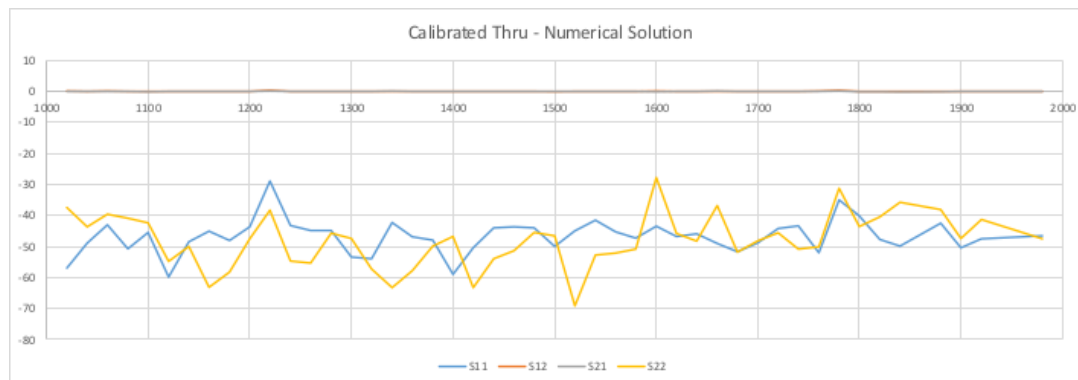
Fig. 5: Result of measuring the 'Thru' calibration standard (a tube of zero-length) using the numerical calibration method. The expected results are perfect transmission (0dB loss) as shown, and zero reflection (-∞ dB). The residual signal shows -40–50dB, representing the noise floor of the system.
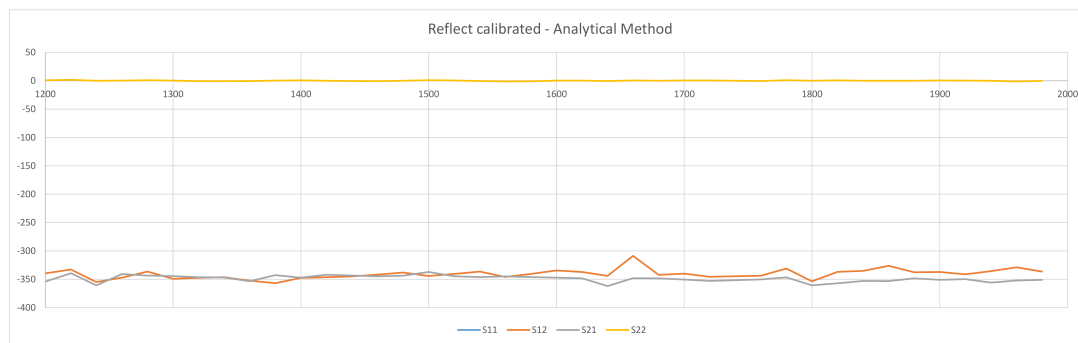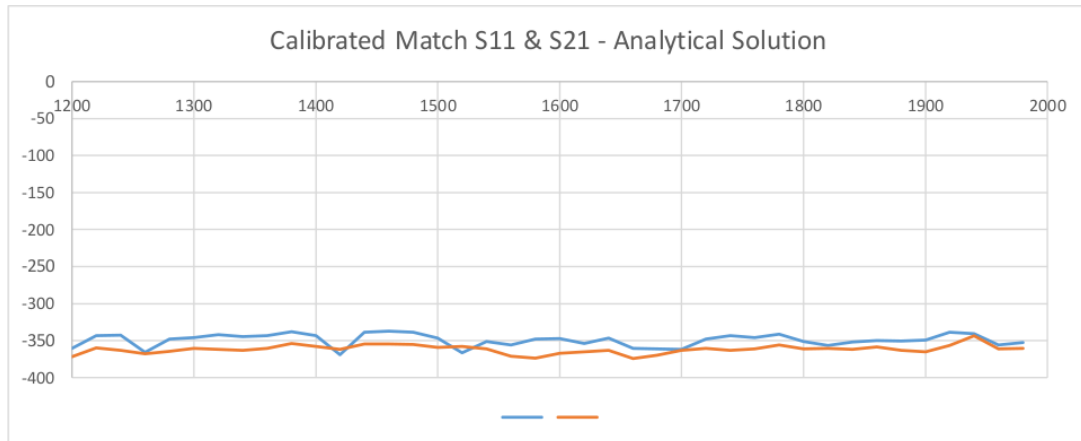

Fig. 6: Result of measuring the 'reflect' calibration standard (a steel plate) using the analytical calibration method. The expected results are perfect perfect reflection (0dB loss) as shown, and zero transmission (-∞ dB). The residual signal is $\approx -350\,\mathrm{dB}$.

In favour of the numerical approach, we may observe that the noise floor gives an indication for the noise in the measurements including those used in the calibration. Further, it can be used in principle with any set of standards or permutations of standards that produces enough information to solve the equations. Against this approach, it tends to give a weaker calibration. While the analytical method is weaker in it's indication of noise, and requires a specific set of standards it does give strong calibrations.

6 Summary

We have built a dual-port acoustic vector network analyser and we have shown an initial calibration. These two steps are crucial to the realization of the vector network analyser as a traceable acoustic measurement system. Further comparison of calibrated results with with a simulation, using Computational Fluid Dynamics (CFD) is required. This characterisation will be of a complicated acoustic waveguide structure, and if our instrument agrees with simulations of that structure, We will pronounce our instrument fully functional. Colleagues at another university are working on simulations currently.

Fig. 7: Result of measuring S_{11} & S_{21} for the 'Match' calibration standard (a sliding load made of open cell foam [29]) using the analytical calibration method. The expected results are zero transmission (-∞ dB), and zero reflection (-∞ dB). The residual signal is $\approx -350\,\text{dB}$.
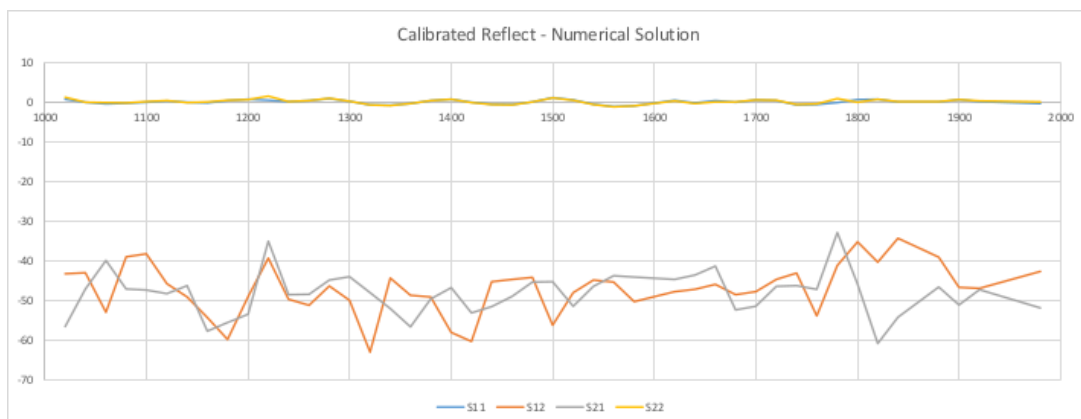
Fig. 8: Result of measuring the 'reflect' calibration standard (a steel plate) using the numerical calibration method. The expected results are perfect reflection (0dB loss) as shown, and zero transmission (-∞ dB). The residual signal shows -40–50dB, representing the noise floor of the system.

$$
\begin{pmatrix}
A_{11} & A_{21} & 0 & 0 & 1 & 0 & 0 & 0 & -M_{a11}A_{11} & -M_{a11}A_{21} & -M_{a12}A_{11} & -M_{a12}A_{21} & -M_{a11} & 0 & -M_{a12} & 0 \\
A_{12} & A_{22} & 0 & 0 & 0 & 1 & 0 & 0 & -M_{a11}A_{12} & -M_{a11}A_{22} & -M_{a12}A_{12} & -M_{a12}A_{22} & 0 & -M_{a11} & 0 & -M_{a12} \\
0 & 0 & A_{11} & A_{21} & 0 & 0 & 1 & 0 & -M_{a21}A_{11} & -M_{a21}A_{21} & -M_{a22}A_{11} & -M_{a22}A_{21} & -M_{a21} & 0 & -M_{a22} & 0 \\
0 & 0 & A_{12} & A_{22} & 0 & 0 & 0 & 1 & -M_{a21}A_{12} & -M_{a21}A_{22} & -M_{a22}A_{12} & -M_{a22}A_{22} & 0 & -M_{a21} & 0 & M_{a22} \\
B_{11} & B_{21} & 0 & 0 & 1 & 0 & 0 & 0 & -M_{b11}B_{11} & -M_{b11}B_{21} & -M_{b12}B_{11} & -M_{b12}B_{21} & -M_{b11} & 0 & -M_{b12} & 0 \\
B_{12} & B_{22} & 0 & 0 & 0 & 1 & 0 & 0 & -M_{b11}B_{12} & -M_{b11}B_{22} & -M_{b12}B_{12} & -M_{b12}B_{22} & 0 & -M_{b11} & 0 & -M_{b12} \\
0 & 0 & B_{11} & B_{21} & 0 & 0 & 1 & 0 & -M_{b21}B_{11} & -M_{b21}B_{21} & -M_{b22}B_{11} & -M_{b22}B_{21} & -M_{b21} & 0 & -M_{b22} & 0 \\
0 & 0 & B_{12} & B_{22} & 0 & 0 & 0 & 1 & -M_{b21}B_{12} & -M_{b21}B_{22} & -M_{b22}B_{12} & -M_{b22}B_{22} & 0 & -M_{b21} & 0 & -M_{b22} \\
C_{11} & C_{21} & 0 & 0 & 1 & 0 & 0 & 0 & -M_{c11}C_{11} & -M_{c11}C_{21} & -M_{c12}C_{11} & -M_{c12}C_{21} & -M_{c11} & 0 & -M_{c12} & 0 \\
C_{12} & C_{22} & 0 & 0 & 0 & 1 & 0 & 0 & -M_{c11}C_{12} & -M_{c11}C_{22} & -M_{c12}C_{12} & -M_{c12}C_{22} & 0 & -M_{c11} & 0 & -M_{c12} \\
0 & 0 & C_{11} & C_{21} & 0 & 0 & 1 & 0 & -M_{c21}C_{11} & -M_{c21}C_{21} & -M_{c22}C_{11} & -M_{c22}C_{21} & -M_{c21} & 0 & -M_{c22} & 0 \\
0 & 0 & C_{12} & C_{22} & 0 & 0 & 0 & 1 & -M_{c21}C_{12} & -M_{c21}C_{22} & -M_{c22}C_{12} & -M_{c22}C_{22} & 0 & -M_{c21} & 0 & -M_{c22} \\
D_{11} & D_{21} & 0 & 0 & 1 & 0 & 0 & 0 & -M_{d11}D_{11} & -M_{d11}D_{21} & -M_{d12}D_{11} & -M_{d12}D_{21} & -M_{d11} & 0 & -M_{d12} & 0 \\
D_{12} & D_{22} & 0 & 0 & 0 & 1 & 0 & 0 & -M_{d11}D_{12} & -M_{d11}D_{22} & -M_{d12}D_{12} & -M_{d12}D_{22} & 0 & -M_{d11} & 0 & -M_{d12} \\
0 & 0 & D_{11} & D_{21} & 0 & 0 & 1 & 0 & -M_{d21}D_{11} & -M_{d21}D_{21} & -M_{d22}D_{11} & -M_{d22}D_{21} & -M_{d21} & 0 & -M_{d22} & 0 \\
0 & 0 & D_{12} & D_{22} & 0 & 0 & 0 & 1 & -M_{d21}D_{12} & -M_{d21}D_{22} & -M_{d22}D_{12} & -M_{d22}D_{22} & 0 & -M_{d21} & 0 & -M_{d22} \\
E_{11} & E_{21} & 0 & 0 & 1 & 0 & 0 & 0 & -M_{e11}E_{11} & -M_{e11}E_{21} & -M_{e12}E_{11} & -M_{e12}E_{21} & -M_{e11} & 0 & -M_{e12} & 0 \\
E_{12} & E_{22} & 0 & 0 & 0 & 1 & 0 & 0 & -M_{e11}E_{12} & -M_{e11}E_{22} & -M_{e12}E_{12} & -M_{e12}E_{22} & 0 & -M_{e11} & 0 & -M_{e12} \\
0 & 0 & E_{11} & E_{21} & 0 & 0 & 1 & 0 & -M_{e21}E_{11} & -M_{e21}E_{21} & -M_{e22}E_{11} & -M_{e22}E_{21} & -M_{e21} & 0 & -M_{e22} & 0 \\
0 & 0 & E_{12} & E_{22} & 0 & 0 & 0 & 1 & -M_{e21}E_{12} & -M_{e21}E_{22} & -M_{e22}E_{12} & -M_{e22}E_{22} & 0 & -M_{e21} & 0 & -M_{e22}
\end{pmatrix}
\begin{pmatrix}
t_0 \\ t_1 \\ t_2 \\ t_3 \\ t_4 \\ t_5 \\ t_6 \\ t_7 \\ t_8 \\ t_9 \\ t_{10} \\ t_{11} \\ t_{12} \\ t_{13} \\ t_{14} \\ t_{15}
\end{pmatrix}
= 0
$$

Fig. 9: Full system of equations. *A* corresponds to the ideal 'Thru' and M_a corresponds to the measured 'Thru', and so on for all standards.

Acknowledgment

References

[1] J. Vieira, "Automatic Estimation of Reverberation Time", in Audio Engineering Society Convention 116, 2004.

[2] J. Vieira, "Estimation of Reverberation Time without Test Signals", in Audio Engineering Society Convention 118, 2005.

[3] P. D'Antonio, T. Cox, "Characterization of Acoustical Materials", Audio Engineering Society Conference: UK 12th Conference: The Measure of Audio (MOA), 1997.

[4] Doug Rytting, "ARFTG 50 year network analyzer history", *71st ARFTG Microwave Measurement Conference*, 20 June 2008, Atlanta, GA, USA.

[5] M. Hiebel, Fundamentals of vector network analysis, 4th ed. Munchen: Rohde & Schwarz, 2008, pp. 15,16.

[6] K. Kurokawa, "Power Waves and the Scattering Matrix", IEEE Transactions on Microwave Theory and Techniques, vol. 13, no. 2, pp. 194-202, 1965. Available: 10.1109/tmtt.1965.1125964 [Accessed 18 July 2019].

[7] ISO 10534-1:1996 Acoustics – Determination of sound absorption coefficient and impedance in impedance tubes – Part 1: Method using standing wave ratio

[8] ISO 10534-2:1998 - Acoustics – Determination of sound absorption coefficient and impedance in impedance tubes – Part 2: Transfer-function method

[9] Pennington, K. (2017). Acoustic Vector Network Analyser (Thesis, Doctor of Philosophy (PhD)). The University of Waikato, Hamilton, New Zealand. Retrieved from `https://hdl.handle.net/10289/11530`

[10] Smith, J., Fritz, C. and Wolfe, J. 'A new technique for the rapid measurement of the acoustic impedance of wind instruments', Proc. Seventh International Congress on Sound and Vibration, July 2000, Garmisch-Partenkirchen, Germany, Vol III, pp.1833?1840.

[11] De Blok, C. M., and R. F. M. Van den Brink, 'Direct-Reading One-Port Acoustic Network Analyzer', Journal of the Audio Engineering Society, vol. 41, no. 4, April 1993, pp231-238.

[12] D. H. Keefe, R. Ling, and J. C. Bulen, 'Method to measure acoustic impedance and reflection coefficient', J. Acoust. Soc. Am., vol. 91, pp. 470?485, January 1992.

[13] Kausel, W., 'Bore reconstruction of tubular ducts from its acoustic input impedance curve', IEEE Transactions on Instrumentation and Measurement, vol. 53, no. 4, August 2004, pp. 1097-1105.

[14] A. Freundorfer, "A coherent optical network analyzer", IEEE Photonics Technology Letters, vol. 3, no. 12, pp. 1139-1142, 1991.

[15] A. P. Freundorfer, "Optical vector network analyzer as a reflectometer," Appl. Opt. 33, 3559-3561 (1994)

[16] V. Adamian, "2-26.5 GHZ On-Wafer Noise and S-Parameter Measurements Using a Solid State Tuner", 34th ARFTG Conference Digest, 1989.

[17] L. Dunleavy, "A Ka-Band On-Wafer S-Parameter and Noise Figure Measurement System", 34th ARFTG Conference Digest, 1989.

[18] A. Davidson, E. Strid and K. Jones, "Achieving greater on-wafer S-parameter accuracy with the LRM calibration technique", 34th ARFTG Conference Digest, 1989.

[19] A. Davidson, K. Jones and E. Strid, "LRM and LRRM Calibrations with Automatic Determination of Load Inductance", 36th ARFTG Conference Digest, 1990.

[20] M. Macdonell, & J. Scott, (2017). Development and Basic Calibration of an Acoustic Vector Network Analyser. Presented at the Electronics New Zealand Conference 2017 (ENZCon 2017), Christchurch, New Zealand, 4-6 December 2017.

[21] Lagasse, P., "Realisation of an acoustical directional coupler", *Journal of sound and vibration*, 15(3), April 1971, pp367–372.

[22] M. MacDonell, 'Scaling acoustic directional couplers using 3D printing', Thesis, Master of Engineering (ME), University of Waikato, 2015.

[23] M. MacDonell, K. Basnet and J. Scott, "Waveguide Joint Design and Validation for use in Acoustic Vector-corrected Network Analysers", 2019 IEEE International Instrumentation and Measurement Technology Conference (I2MTC), Auckland, New Zealand, 2019, pp. 879-883.

[24] Mason and Zimmerman, Electronic Circuits, Signals & Systems, Wiley, 1960.

[25] Kuhn, 'Signal Flow Graphs', Microwave Journal, November 1963, pp 59+.

[26] H. C. Heyker, 'The Choice of Sliding Load Positions to Improve Network Analyzer Calibration', 12th European Microwave Conference, Helsinki, September 1982, pp429-434.

[27] K. Silvonen, "LMR 16-a self-calibration procedure for a leaky network analyzer", IEEE Transactions on Microwave Theory and Techniques, vol. 45, no. 7, pp. 1041-1049, 1997.

[28] J. Butler, D. Rytting, M. Iskander, R. Pollard and M. Vanden Bossche, "16-term error model and calibration procedure for on-wafer network analysis measurements", IEEE Transactions on Microwave Theory and Techniques, vol. 39, no. 12, pp. 2211-2217, 1991.

[29] Scott, J. and K. E. Pennington, "Acoustic Vector-Corrected Impedance Meter", *IEEE Transactions on Instrumentation and Measurement*, 2014. DOI: 10.1109/TIM.2014.2327474

[30] G. Taubin, "Estimation of planar curves, surfaces, and nonplanar space curves defined by implicit equations with applications to edge and range image segmentation," IEEE Trans. Pattern Anal. Mach. Intell., vol. 13, no. 11, pp. 1115–1138, Nov. 1991.